Evaluating Pressure Swing Adsorption as a CO_2 separation technique in coal-fired power plants

Luca Riboldi[a,1], Olav Bolland[a]

[a]*Energy and Process Engineering Department, the Norwegian University of Science and Technology, NO-7491Trondheim, Norway*

Abstract

The paper provides with a first assessment on the suitability of Pressure Swing Adsorption (PSA) as a valid option for Carbon Capture and Storage (CCS) in coal-fired power plants. A full-plant analysis of an Advanced SuperCritical (ASC) pulverized coal plant and of an Integrated Gasification Combined Cycle (IGCC) plant, operating with a PSA unit, is presented. The systems selected aim to represent the most diffused options for coal-based power generation, respectively in a post- and pre-combustion application of CO_2 separation. The definition of the PSA process is tailored for the two different scenarios considered, starting from the adsorbent selected (zeolite 5A and activated carbon, respectively for post- and pre-combustion). The objective is to investigate the competitiveness of PSA with respect to the benchmark technology for CCS, namely absorption. In order to consider the different aspects measuring the effectiveness of a CO_2 separation technique, the performance of the power plants is evaluated in terms of CO_2 separation performance, energy efficiency and footprint of the technology. The post-combustion scenario analysis shows that PSA can be competitive with regard to the separation and the energy performance. PSA is able to match the CO_2 separation requirements, and the relative energy penalty is slightly lower than that resulting from amine-absorption. Despite that, the footprint of the PSA unit demonstrates to be way larger than that related to absorption and unlikely acceptable.

PSA in the pre-combustion scenario returns encouraging results, approaching the outcomes achieved with absorption both in terms of CO_2 separation performance and plant energy efficiency. The footprint, even though significantly larger, appears to be reasonable for actual implementation.

Keywords: CO_2 capture; Process simulations; Coal-fired power plants; Pressure Swing Adsorption; Efficiency penalty.

1. Introduction

The atmospheric concentration of carbon dioxide (CO_2) has increased by 40% since pre-industrial times, and recently passed the 400 ppm milestone. CO_2 is regarded as the main responsible for the atmospheric greenhouse effect, which is producing the warming of the climate system. It is extremely likely that human influence has been the dominant cause of the observed warming [1]. One possible mitigation action for stabilizing the atmospheric CO_2 concentration, while continuing exploiting fossil fuel resources, is Carbon dioxide Capture and Storage (CCS). CCS consists in separating CO_2 from large anthropogenic point sources, such as thermal power plants, compressing it for transportation and permanently storing it in underground geological formation. There are different types of CO_2 capture systems: post-combustion, pre-combustion and oxyfuel combustion [2]. Many different techniques have been proposed for capturing CO_2. These includes: chemical or physical absorption, adsorption, reactive solids, membranes, cryogenic processes [3]. To date, all commercial CO_2 capture plants are based on absorption for separating CO_2 [4], as it is the most mature and well understood technology. However, its large scale deployment is hindered by the large power consumption, which negatively affects the energy efficiency of the plant. That, summed to other concerns related to the solvent toxicity and to the potentially high corrosion

[1] Corresponding author. Tel.: +47 735 93559;
E-mail address: luca.riboldi@ntnu.no (L. Riboldi)

rate, makes advisable to investigate alternatives. In the current work, Pressure Swing Adsorption (PSA) process is analyzed as an option for post- and pre-combustion CO_2 capture. PSA is a cyclic process. During the adsorption step, the CO_2 present in the feed gas stream is fixed on the surface of the selected adsorbent. Following, the regeneration of the bed is carried out by a pressure swing operation. The potential advantage connected to this process is the absence of any thermal energy duty during the regeneration step. Adsorption processes have been successfully employed for CO_2 removal from synthesis gas for hydrogen production [5-9]. With regard to CCS applications, PSA process suitability has to be proven yet. A large number of studies have been done in order to assess PSA processes operating in the condition typical of post- [10-24] and pre-combustion [25, 26] applications. A significant lack was found in the analysis of more comprehensive systems [27], where the PSA process is integrated with the rest of the plant. Few works deal with the understanding of such complex arrangements. In post-combustion applications, only preliminary studies have been carried out, whose results can be considered partial [28] and/or focusing on a particular side of the topic (e.g., economic considerations) [29]. In pre-combustion applications, more thorough analyses have been performed. Liu and Green [30] evaluated the applicability of PSA as CO_2 removal technology in an Integrated Gasification Combined Cycle (IGCC). They simulated a warm PSA process based on a tailored adsorbent, able to perform at elevated temperature. The results achieved are in line with those of a Selexol absorption process. Other studies investigated the performance of Sorption Enhanced Water Gas Shift (SEWGS), an innovative CO_2 capture process for pre-combustion applications, applied to both IGCC [31] and Natural Gas Combined Cycle (NGCC) [32]. In either case the outcome appears to be extremely promising. The objective of this paper is to provide a full-plant analysis of coal-fired plants implementing CO_2 capture by a cold PSA process, meaning that the process takes place at temperature levels suitable for many of the most common adsorbents. Coal was selected as fuel because of its higher emission index (higher CO_2 emission per unit of energy released). Further, coal utilization is predicted to increase in the future, under any foreseeable scenario [27]. Thus, CCS will become a critical tool in order to enable a sustainable exploitation of coal. Two plant configurations were considered, respectively to account for a post- and a pre-combustion scenario. Post-combustion CO_2 capture is implemented by integrating a PSA process into an Advanced SuperCritical (ASC) pulverized coal plant. Pre-combustion CO_2 capture is implemented by integrating a PSA process into an Integrated Gasification Combined Cycle (IGCC) plant. First, the layout of the thermal power plant, to be coupled with the CO_2 capture unit, is defined and modeled. Following, the modeling of the PSA process is presented resulting in a dynamic computational model. The procedure for the choice of the optimal PSA process configuration is outlined. A full-plant analysis is then provided for both the scenarios. Simulations were also implemented for the reference case without CO_2 capture and for the case with CO_2 capture based on an absorption process. A plant-level comparison is carried out, returning the competitiveness of PSA process with regard to another technique of decarbonization (i.e., state-of-the-art absorption processes). The performance of the system is evaluated on three levels, namely CO_2 separation performance, energy efficiency and footprint of the technology.

2. Modeling of the power plant

The model of the power plant was developed by Thermoflow Inc. products: STEAM PRO, GT PRO and THERMOFLEX. The focus is on coal-fired power plants, since combustion of coal produces high specific emission of CO_2 per unit of electricity generated. Accordingly, two thermal power plant layouts were selected to represent the most common systems for coal-based power generation. These systems are an Advanced SuperCritical (ASC) pulverized coal plant and an Integrated Gasification Combined Cycle (IGCC) plant, respectively constituting the basis for the post- and pre-combustion CO_2 capture scenario.

First, a baseline case without CO_2 capture was modeled. The purpose was to benchmark the coal-fired power plant, in order to have a reference case for comparisons. However, the object of the study is to assess the plant performance when CO_2 capture is implemented. Therefore, the mentioned plants were equipped with a CO_2 capture unit. A mature technology for separating CO_2 from the gas stream already exists (i.e., absorption). For the sake of fair comparisons between different CO_2 capture technologies, models were developed for the plants with state-of-the-art absorption CO_2 capture processes. For the post-combustion scenario, a MEA-based chemical absorption process was considered. For the pre-combustion scenario, a Selexol-based two-stage absorption process was considered. Finally, the same power plants coupled to a PSA process for CO_2 capture were modeled, as this constitutes the core of the current work. Six cases were, hence, simulated:

1. ASC plant without CO_2 capture
2. ASC plant with CO_2 capture by absorption
3. ASC plant with CO_2 capture by PSA
4. IGCC plant without CO_2 capture
5. IGCC plant with CO_2 capture by absorption
6. IGCC plant with CO_2 capture by PSA

All the cases discussed were based on the European Benchmarking Task Force (EBTF) recommendations [33]. The purpose was to define a common set of assumptions and parameters for the different simulations, in order to guarantee the consistency of the comparisons. A description of the reference coal-fired power plants and of the same plants implementing CO_2 capture by absorption can be found in the EBTF report [33]. In the present work, only the definition of the additional units in the plant layout integrating a PSA process is reported, as this constitutes the novelty of the analysis.

2.1. ASC plant with CO_2 capture by PSA

The integration of a PSA unit in the ASC plant is not affecting much the general layout. The additional units are all downstream the flue gas treatment units, and consist in a water removal section, a PSA process and a compression stage for CO_2 transport. The plant upstream remains basically unchanged. The resultant plant layout is represented in **Figure 1**. The characteristics of the most relevant streams are given in **Table 1**.

The water removal unit is added because water is known to hinder the CO_2 adsorption process. An equilibrium separation is carried out. The flue gas stream is cooled down to approximately 20°C and fed to a flash separator. This simple process can only lower the water content down to about 2%. It would be advisable to reach water contents much lower than that, but it would require a different dehydration strategy. This has not been included in the simulation. For a deeper insight regarding the water presence issue, refer to the dedicated section *3.3*. The partially dehydrated flue gas stream is entering the PSA unit, where CO_2 is separated from the other components in a two stages PSA process. The necessity of two PSA stages will be illustrated later. The pressure of the CO_2-rich gas stream leaving the PSA unit needs to be raised to an appropriate level for transportation and storage. A target pressure of 110 bar was assumed. The CO_2-rich stream undergoes a compression process in a five-stage intercooled compressor. The CO_2-lean stream resulting from the PSA process is vented to the atmosphere.

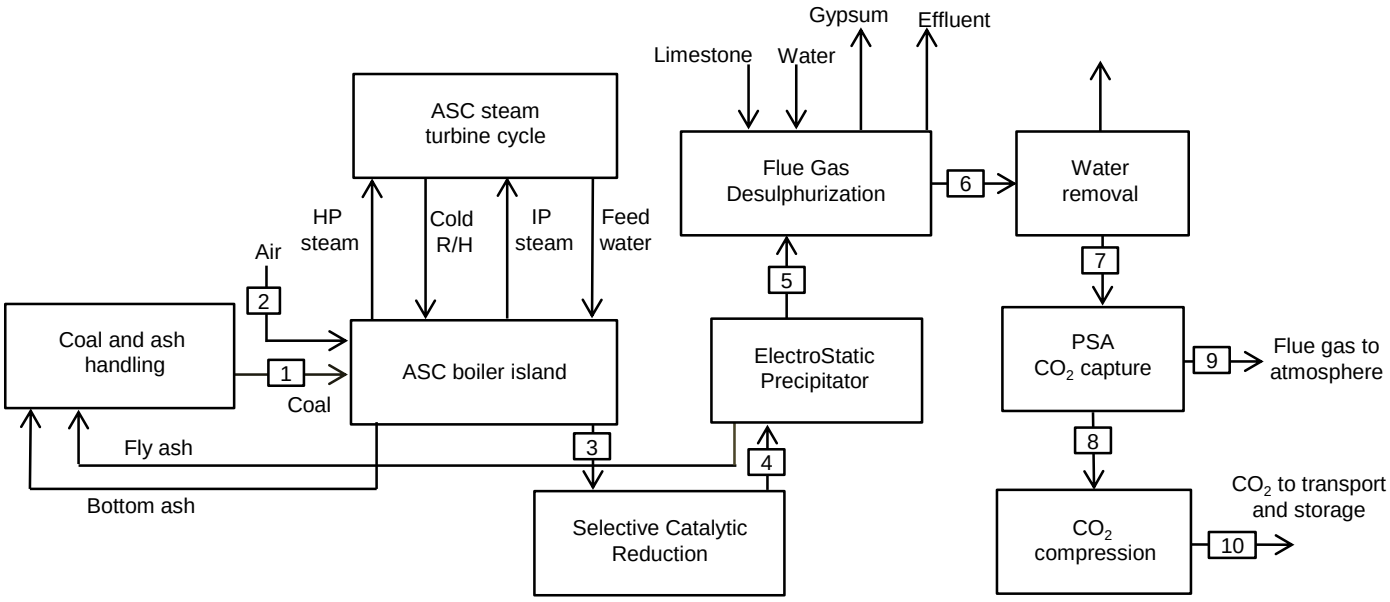

Figure 1. ASC plant with integrated a PSA unit for CO_2 capture and a CO_2 compression unit.

Table 1. Stream table of the ASC plant with integrated a PSA unit for CO_2 capture and a CO_2 compression unit.

Stream	ṁ	T	P	MW	Composition (% mol.)					
	kg/s	°C	bar	g/mol	CO_2	N_2	O_2	Ar	SO_2	H_2O
1	66,2	25,0	1,0	-	-	-	-	-	-	-
2	744,2	15,0	1,0	28,9	0,03	77,3	20,7	0,9	-	1,0
3	735,7	338,9	1,0	29,9	14,9	74,1	2,9	0,9	0,04	7,2
4	800,8	117,0	1,0	29,8	13,6	74,4	4,4	0,9	0,04	6,7
5	800,8	127,1	1,0	29,8	13,6	74,4	4,4	0,9	0,04	6,7
6	823,3	62,5	1,0	29,3	13,1	71,3	4,2	0,9	0,002	10,5
7	781,1	20,0	1,0	30,4	14,3	77,8	4,6	0,94	0,002	2,3
8	150,4	15,4	1,0	43,2	95,1	4,6	0,3	0,02	-	-
9	619,7	35,2	1,0	28,6	1,7	91,8	5,4	1,1	-	-
10	150,4	28,0	110,0	43,2	95,1	4,6	0,3	0,02	-	-

2.2. IGCC plant with CO_2 capture by PSA

The addition of a PSA unit to the IGCC plant requires a higher degree of integration compared to the post-combustion scenario. A major difference is that the CO_2-lean gas stream leaving the PSA process (i.e., the H_2-rich gas stream) is further processed in the plant, constituting the fuel for the gas turbine. The additional units, with respect to the reference IGCC plant [33], consist in a water-gas shift section, a PSA process and a compression stage for CO_2 transport. The plant layout is represented in **Figure 2**. The characteristics of the most relevant streams are given in **Table 2**.

The Water-Gas Shift (WGS) converts CO and H_2O into CO_2 and H_2, providing a beneficial effect on the following CO_2 separation due to the increase in the CO_2 partial pressure. COS hydrolysis is also carried out in the WGS process. The syngas is then cooled down. During the cooling process, condensing water is removed. Thanks to the relatively high pressure, water presence is drastically decreased (≈ 0.6%). The syngas stream at an appropriate temperature is fed to the H_2S removal unit and successively to the PSA unit. The outputs of the PSA process are a CO_2-rich stream and a H_2-rich stream. The latter is the fuel for the gas turbine cycle and is preheated by the syngas leaving the WGS process. Since the CO_2-rich gas stream does not achieve the requirements for being processed and transported, a further purification step is implemented. It consists in the removal of impurities by means of two flash separators integrated in the CO_2 compression section (see **Figure 3**). This approach has already been suggested for removing a selection of non-CO_2 gases from oxy-combustion power plants [34, 35]. After a first partial compression (up to 30 bar) and a dehydration process, the CO_2-rich gas stream enters a system of two multi-stream heat exchangers, each followed by a flash separator. The appropriately set temperature levels (-30°C and -54.5°C [35]) allow to separate two different streams: a CO_2-rich stream, matching the requested purity specifications, which completes the compression process; a CO_2-lean stream, rich in H_2, which can be added to the syngas injected as fuel in the gas turbine. The CO_2-rich stream is further compressed to 110 bar in an intercooled-compressor. An air expander is also present, providing an additional power output. It partially expands the air extracted from the gas turbine compressor and fed to the ASU, in order to recover part of the compression work.

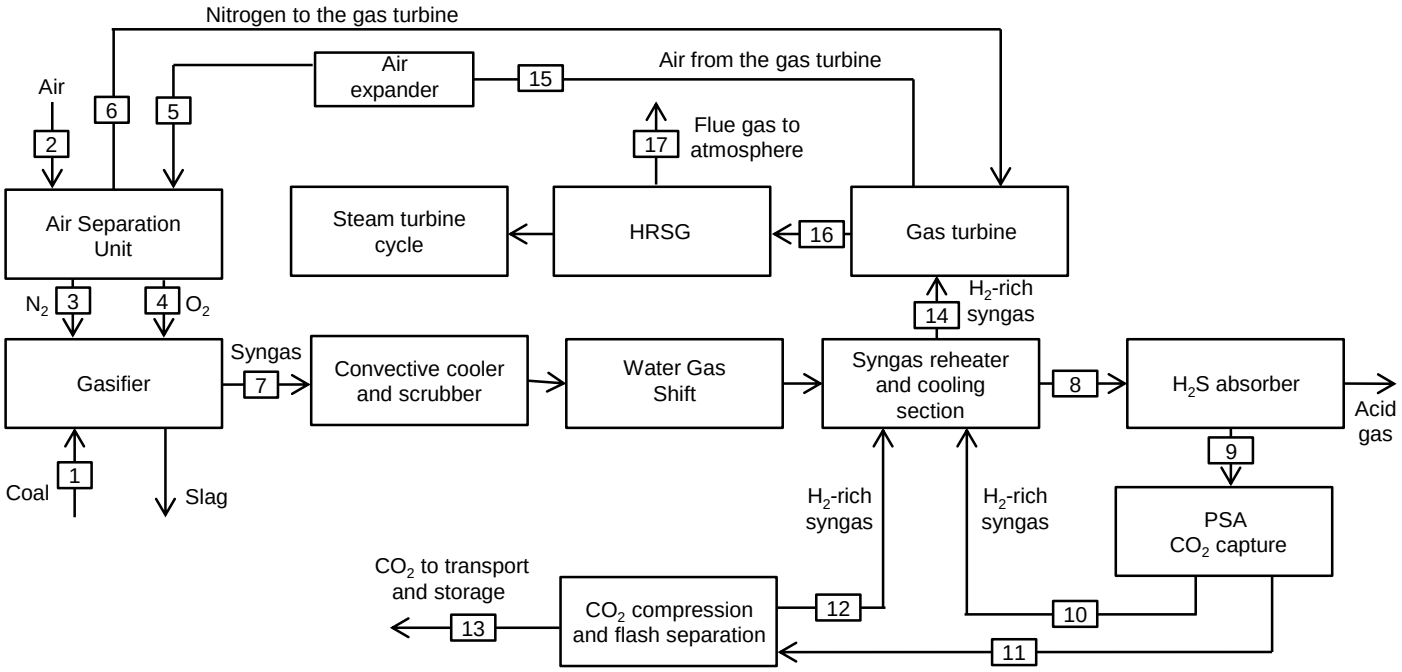

Figure 2. IGCC plant with integrated a PSA unit for CO_2 capture and a CO_2 compression unit.

Table 2. Stream table of the IGCC plant with integrated a PSA unit for CO_2 capture and a CO_2 compression unit.

Stream	ṁ	T	P	MW	Composition (% mol.)								
	kg/s	°C	bar	g/mol	H_2	CO_2	CO	CH_4	N_2	O_2	Ar	H_2S	H_2O
1	38,5	25,0	1,0	7,7	-	-	-	-	-	-	-	-	-
2	64,6	15,0	1,0	28,9	-	0,03	-	-	77,3	20,7	0,9	-	1,0
3	8,5	82,5	1,0	8,5	-	0	-	-	100	-	-	-	-
4	31,2	123,9	44,9	32,0	-	0	-	-	3,5	95,0	1,5	-	-
5	64,6	351,8	10,6	28,9	-	0,03	-	-	77,3	20,7	0,9	-	1,0
6	87,5	116,2	24,1	28,0	-	0	-	-	100	-	-	-	-
7	76,3	497,1	43,1	21,3	26,2	3,1	55,7	-	10,0	-	0,4	0,2	4,3
8	108,7	47,2	39,4	20,2	53,1	37,7	1,5	0,06	6,7	-	0,3	0,1	0,6
9	107,6	64,0	38,8	20,2	53,5	37,9	1,5	0,06	6,7	-	0,3	0,0001	0,03
10	19,1	62,5	38,8	6,5	84,7	2,6	2,0	0,1	10,1	-	0,5	-	-
11	88,6	38,6	1,0	37,2	14,8	81,6	0,9	0,03	2,5	-	-	-	0,06
12	8,2	17,6	27,7	15,1	63,5	22,8	3,5	0,1	10,0	-	-	-	-
13	80,4	28,0	110,0	43,7	0,6	98,9	0,1	0,01	0,4	-	-	-	-
14	27,2	230,0	24,1	7,8	81,5	5,7	2,2	0,08	10,1	-	0,4	-	-
15	64,6	432,3	17,6	28,9	-	0,03	-	-	77,3	20,7	0,9	-	1,0
16	656,1	579,5	1,0	27,4	-	1,2	-	-	75,1	10,1	0,8	-	12,7
17	656,1	113,8	1,0	27,4	-	1,2	-	-	75,1	10,1	0,8	-	12,7
18	88,5	28,0	30,0	37,2	14,8	81,7	0,9	0,03	2,6	-	-	-	-
19	88,5	-30,0	30,0	37,2	14,8	81,7	0,9	0,03	2,6	-	-	-	-
20	24,5	-54,5	28,8	26,9	37,7	54,0	2,2	0,07	6,1	-	-	-	-
21	16,4	17,7	7,2	43,7	0,6	98,8	0,2	0,01	0,5	-	-	-	-
22	64,0	17,7	17,4	43,7	0,6	99,0	0,1	0,01	0,3	-	-	-	-

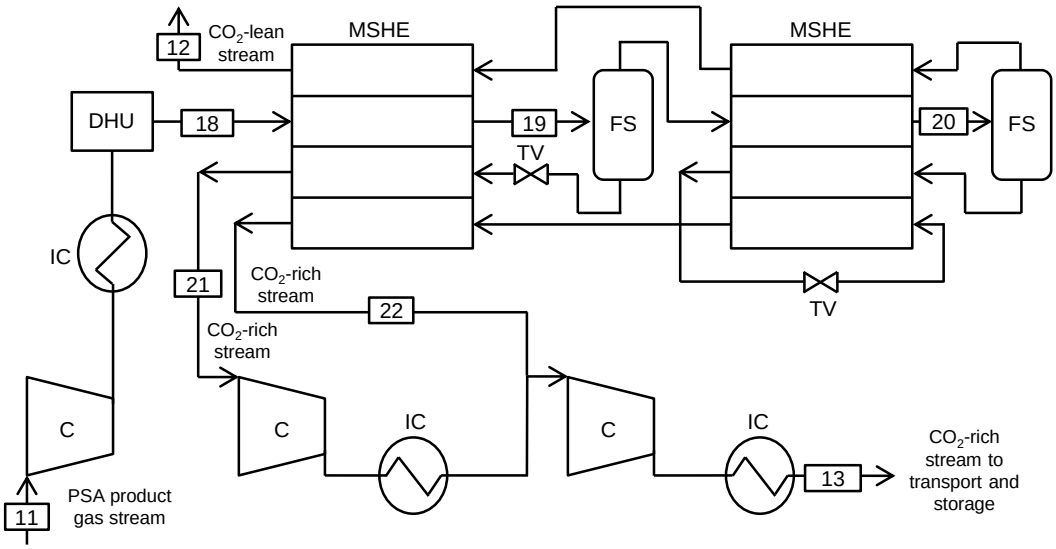

Figure 3. CO_2 compression unit integrated with a double flash separation process.

3. Modeling of the PSA unit

3.1. Adsorption bed model

The mathematical model for the dynamic simulation of an adsorption bed relies on material, energy and momentum balances. The adsorbents are considered to have a bi-disperse structure (i.e., a population of macro and micropores). Three material balances would be theoretically necessary, one for the bulk gas phase, one for the macropores and one for the micropores. In order to reduce the computational time requested to solve the set of equations, a simplification was introduced. This simplification is based on the evaluation of the mass transfer resistances, and it assumes the limiting case where one mass transfer mechanism is controlling, namely the diffusion in the micropores. Accordingly, the other mass transfer resistances have been neglected (i.e., macropore and film diffusion). This simplification have been supported by previous studies [36-38] and have been already successfully applied by other works simulating the behavior of PSA units [6, 25]. The kinetic of the mass transfer process is accounted for the Linear Driving Force (LDF) approximation [39-42]. Its application is in line with the material balance simplifications above-mentioned. Similarly the energy balances have been simplified assuming thermal equilibrium between the gas and solid phases, reducing to one the equation needed [6]. An energy balance with the wall and the environment should be considered. It is common practice to describe the heat transfer with the wall and the environment by average heat transfer coefficients. However, the influence of these terms is decreasing with the size of the unit. Given that the novelty of this work is to evaluate the PSA unit performance in actual operating arrangements (large diameter reactors and large gas flow rates), the reactors have been considered to be adiabatic. This approach seems to provide satisfactory predicting capabilities and it simplifies the model. The additional assumptions adopted in the model are listed below:

- The gas in the bulk phase is considered to follow the ideal gas law.
- The bed is assumed uniform throughout all its length (10 m). Constant bulk density (735 kg/m^3 for the zeolite 5A and 522 kg/m^3 for the activated carbon) and bed porosity (0.32 for the zeolite 5A and 0.38 for the activated carbon).
- The flow pattern is described by the axially dispersed plug flow.
- The radial diffusion effects are ignored.
- The momentum balance is described by the use of the well-known Ergun equation [43].
- The heat of adsorption is independent of temperature and adsorbed phase loading.

Based on these assumptions, the governing equations utilized are the following.

Component mass balance:

$$\frac{\partial C_i}{\partial t}\left[\varepsilon+\varepsilon_p(1-\varepsilon)\right]=-\frac{\partial(u_s C_i)}{\partial z}+\frac{\partial}{\partial z}\left(\varepsilon D_{ax,i}C_i\frac{\partial y_i}{\partial z}\right)-\rho_p(1-\varepsilon)\frac{\partial \bar{q}_i}{\partial t} \quad (1)$$

LDF model:

$$\frac{\partial \bar{q}_i}{\partial t}=k_{LDF,i}\left(q_i^*-\bar{q}_i\right) \quad \text{with} \quad k_{LDF,i}=\chi_{LDF}\frac{D_{c,i}}{r_c^2} \quad (2)$$

Overall mass balance:

$$\frac{\partial C_{tot}}{\partial t}\left[\varepsilon+\varepsilon_p(1-\varepsilon)\right]=-\frac{\partial(u_s C_{tot})}{\partial z}-\rho_p(1-\varepsilon)\sum_i^{NC}\frac{\partial \bar{q}_i}{\partial t} \quad (3)$$

Energy balance:

$$\left[\varepsilon C_{p,G}C_{tot}+\varepsilon_p(1-\varepsilon)C_{p,G}C_{tot}+(1-\varepsilon)C_{p,S}\rho_p+(1-\varepsilon)\rho_p\sum_i^{NC}C_{p,ads,i}\bar{q}_i\right]\frac{\partial T}{\partial t}=-u_s C_{p,G}C_{tot}\frac{\partial T}{\partial z}+$$
$$+\frac{\partial}{\partial z}\left(\lambda_{ax}\frac{\partial T}{\partial z}\right)+\rho_p(1-\varepsilon)\sum_i^{NC}\left(-\Delta H_{r,i}\right)\frac{\partial \bar{q}_i}{\partial t} \quad (4)$$

Momentum balance:

$$\frac{\partial P}{\partial z}=-\left[\frac{150}{d_p^2}\frac{(1-\varepsilon)^2}{\varepsilon^3}\mu u_s+\frac{1.75}{d_p}\frac{(1-\varepsilon)}{\varepsilon^3}\rho_G u_s|u_s|\right] \quad (5)$$

The transport parameters are evaluated through frequently used correlations (see **Table 10** in Appendix A). Averaged values were successively used for the simulations. Physical properties of the gas were evaluated in all the points of the bed through an external physical property package (i.e., Multiflash – Infochem Computer Services Ltd) interfaced with the main simulation tool.

The adsorbent selected for the post-combustion scenario is a zeolite 5A [44]. Zeolites are well studied CO_2 adsorbents, which proved to perform well in the conditions typical of post-combustion applications (i.e., very low CO_2 partial pressure) [45-47]. Even though zeolites 13X are normally regarded as the most effective zeolites for CO_2 adsorption processes, a zeolite 5A was considered. This choice was driven by the availability of data and comparative results [16]. Bearing in mind that the simulation outputs would possibly be slightly superior with a zeolite 13X, it is opinion of the authors that the key outcomes presented afterwards are still valid. The same considerations can be applied discussing the possibility of utilizing two different adsorbents in the two PSA stages. Tailored adsorbents can suit better the specific operating conditions providing a performance enhancement but hardly significant.

The uptake capacity of the adsorbent is described by an extended multi-site Langmuir model:

$$\frac{q_i^*}{q_{m,i}} = a_i k_i P_i \left[1 - \sum_i^{NC} \left(\frac{q_i^*}{q_{m,i}} \right) \right]^{a_i} \quad \text{, with } \; k_i = k_{\infty,i} \exp\left(-\frac{\Delta H_{r,i}}{RT} \right) \tag{6}$$

Data were available just for CO_2 and N_2, the main constituents of the flue gas to process. The fraction of O_2 has been included with N_2. This approximation has been suggested by the similar selectivity of CO_2 with regards to N_2 and O_2 [11, 45] and it is therefore thought not to meaningfully affect the results.

The adsorbent selected for the pre-combustion scenario is an activated carbon [36]. Activated carbons demonstrated to outperform zeolites when overpassing a certain threshold (≈ 7 bar) of CO_2 partial pressure [45]. Thus, in the typical pre-combustion operating conditions (e.g., P_{CO2} = 14.7 bar) activated carbon has been considered to be the most suitable option. The adsorption isotherm was again described by an extended multi-site Langmuir model, represented by equation (6). Even though equilibrium data were available also for CH_4, the syngas components given as an input in the PSA model were just CO_2, H_2, CO and N_2. The small mole fraction of methane would not really influence the performance of the whole unit. Nevertheless, adding another component resulted in less stability of the model and additional computational efforts. Thus, the fraction of CH_4 has been included with CO.

The physical properties, the kinetic and the equilibrium data of the adsorbents are reported in **Table 3**.

Table 3. Bed characteristics, physical properties, kinetic data equilibrium data of the adsorbents.

Physical properties						
		d_p (mm)	ε_p	ρ_p (kg/m3)	$C_{p,s}$ (J/kg/K)	
Zeolite 5A [44]		2,70	0,30	1083	920	
Activated carbon [36]		2,34	0,57	842	709	
Equilibrium and kinetic parameters						
	a (-)	k_∞ (Pa^{-1})	q_m (mol/kg)	ΔH_r (kJ/mol)	D^0_c/r_c^2 (s^{-1})	E_a (kJ/mol)
Zeolite 5A [44]						
CO_2	2,1	1,47E-11	3,92	-37,9	14,8	26,3
N_2	2,5	3,79E-11	3,28	-19,4	0,1	6,3
Activated carbon [36]						
CO_2	3,0	2,13E-11	7,86	-29,1	17,5	15,8
N_2	4,0	2,34E-10	5,89	-16,3	1,0	7,0
H_2	1,0	7,69E-11	23,57	-12,8	14,8	10,4
CO	2,6	2,68E-11	9,06	-22,6	59,2	17,5

3.2. PSA process

PSA is a gas separation process in which the adsorbent is regenerated by rapidly reducing the partial pressure of the adsorbed component, either by lowering the total pressure or by using a purge gas. The process is inherently discontinuous, since during the regeneration step the gas feed to a column has necessarily to be interrupted. Thus, different columns working in tandem are requested in order to enable the processing of a continuous feed. A coordinated group of columns is defined as PSA train. If different trains are present, the process gas stream is equally split between them. The columns of a train cyclically undergo a series of steps in an asynchronous manner. Some of these steps are closely interconnected, implying restrictions to the scheduling of the cycle. The steps that have been considered for the PSA process are:

- Feed (F): the feed gas is co-currently injected at the bottom of the column. The components of the gas stream starts to be selectively adsorbed on the surface of the adsorbent.
- Rinse (R): before starting the regeneration of the bed, part of the product gas is fed to the column. This gas, rich in CO_2, displaces the inert bulk gas remained in the column after the feed step.

- Depressurization (D): the pressure is reduced by putting in contact the column with another at a lower pressure level.
- Blowdown (BD): the pressure is reduced to the lowest level in order to regenerate the bed. A stream of CO_2-rich gas is leaving the column during this step.
- Purge (Pu): the regeneration is completed by injecting a purging gas into the column, normally counter-currently. This step is again carried out at the lowest pressure of the system and produces a CO_2-rich gas stream.
- Pressurization (P): the pressure is increased by putting in contact the column with another at a higher pressure level.
- Null (N): the column is left idle.
- Feed Pressurization (FP): part of the feed gas is used to pressurize the column to the highest pressure level necessary for the adsorption process.

The different operating conditions in which the PSA process is supposed to perform in post- and pre-combustions scenarios, necessarily led to different configurations, in terms of number of beds and type of steps. The guiding criterion, for the selection of the process layout, was the necessity of approaching values of CO_2 recovery and purity sufficient for a CCS application (i.e., CO_2 recovery ≈ 90% and purity ≈ 95%). A multitude of different process configurations exists and may be employed. Given the large number of variables to consider (i.e., type and number of steps, duration of the cycle, adsorbent material, etc.) there is not a well-defined framework to pinpoint the most suitable alternative. In the present work, it was decided to refer to cycle configurations successfully employed in the literature [16, 25]. Minor changes have been done with respect to those cycles, in order to deal with the slightly different operating conditions considered. However, other configurations are possible and may lead to similar good performance. For the post-combustion scenario, a first PSA stage consists in a three-bed five-step cycle, while a second stage consists in a two-bed five-step cycle. The sequence of different steps undergone by a column is shown in **Figure 4**. For the pre-combustion scenario, the PSA configuration adopted in the present work is a seven-bed twelve-step cycle, where the sequence of different steps undergone by a column is shown in **Figure 5**.

Different boundary conditions have to be established for each step of the PSA cycle. The Danckwerts boundary conditions are applied. They assume no dispersion or radial variation in concentration or temperature either upstream or downstream of the reaction section. **Table 11** in the Appendix B reports those boundary conditions.

The energy consumption directly related to the PSA process consists in the power necessary to a fan to overcome the pressure drops and the power necessary to the vacuum pump to create an under-atmospheric pressure (when requested from the regeneration process). If a rinse step is implemented, a fan is necessary for feeding the rinse flow rate into the column and overcoming the pressure drops. Furthermore, a gas compression may be applied, with the relative compression power duty. These energy consumptions were evaluated within the PSA model as following:

$$\text{Fan power} = \frac{1}{\eta_{is}} \frac{\gamma_{fan}}{\gamma_{fan} - 1} R\, T_{in} \left[\left(\frac{P_{in}}{P_{out}} \right)^{\frac{\gamma_{fan}-1}{\gamma_{fan}}} - 1 \right] \dot{n}_{in} \tag{7}$$

$$\text{Compressor power} = \frac{1}{\eta_{is}} \frac{\gamma_{compr}}{\gamma_{compr} - 1} R\, T_{in} \left[\left(\frac{P_{in}}{P_{out}} \right)^{\frac{\gamma_{compr}-1}{\gamma_{compr}}} - 1 \right] \dot{n}_{in} \tag{8}$$

$$\text{Vacuum power} = \frac{1}{\eta_{is}} \frac{\gamma_{vacuum}}{\gamma_{vacuum} - 1} R\, T_{in} \left[\left(\frac{P_{atm}}{P_{out}} \right)^{\frac{\gamma_{vacuum}-1}{\gamma_{vacuum}}} - 1 \right] \dot{n}_{in} \tag{9}$$

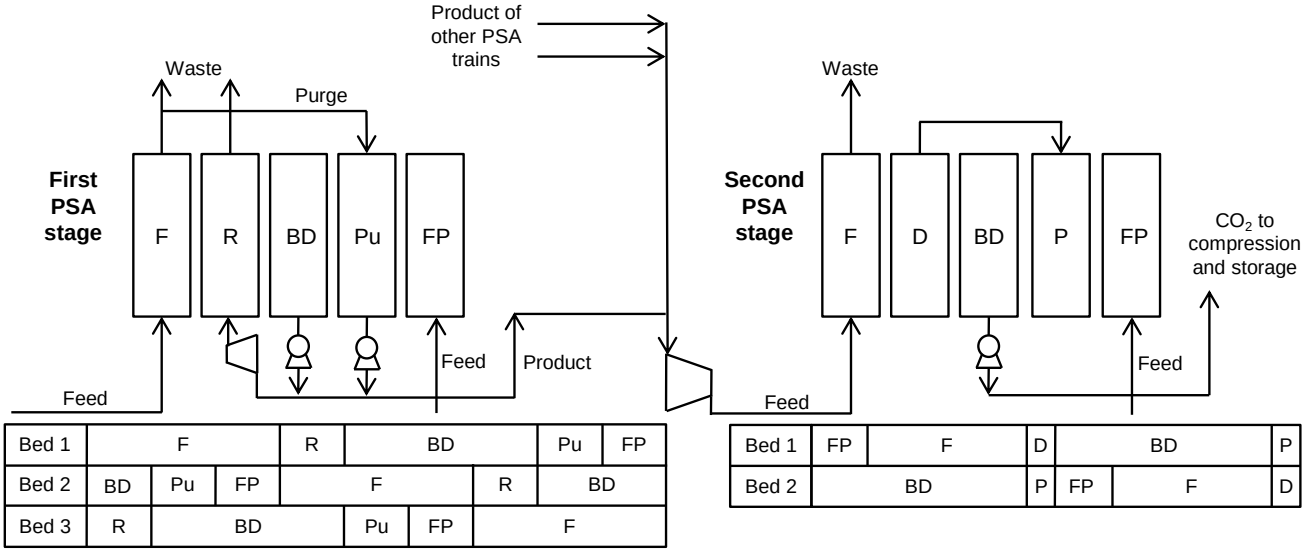

Figure 4. PSA processes for the post-combustion scenario. Representation of the sequence of steps undergone by a single column in the first and second PSA stage.

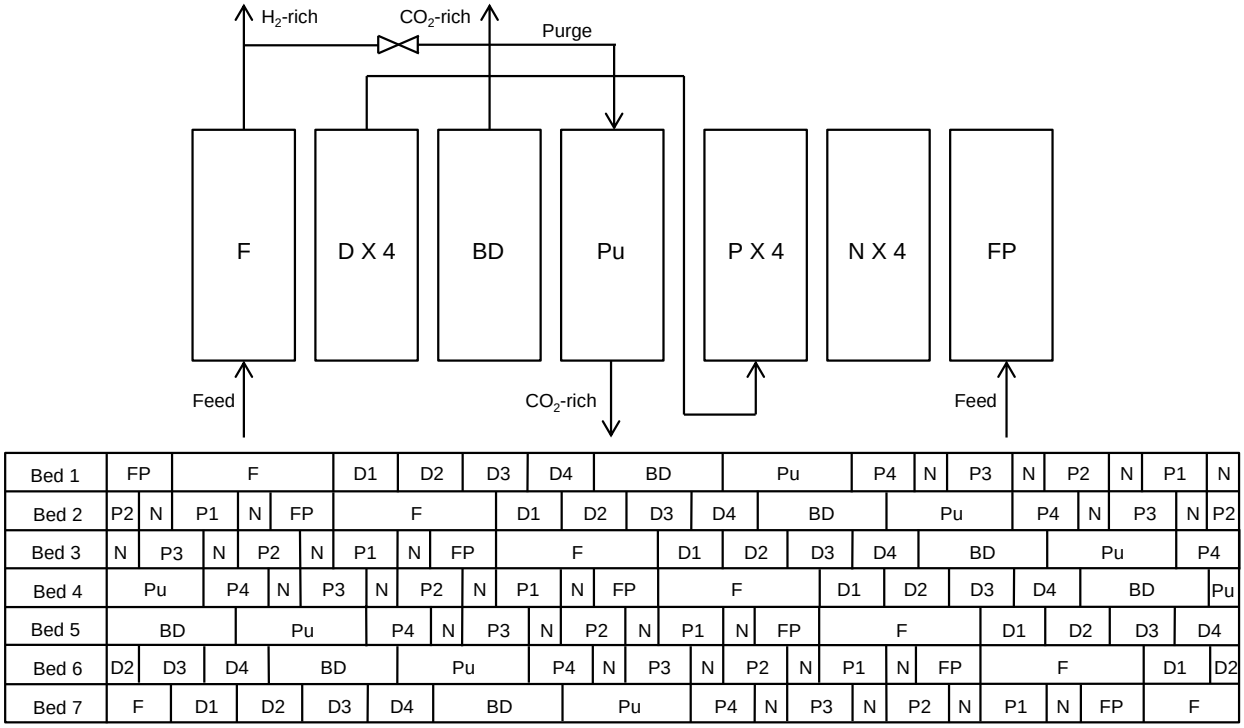

Figure 5. PSA process for the pre-combustion scenario. Representation of the sequence of steps undergone by a single column.

3.3. Water and adsorption

Presence of water is often troublesome in PSA processes. Water competitively adsorb on the solid sorbents and tend to accumulate since classical pressure swing operation may be not sufficient to desorb it. Both zeolites and activated carbons have demonstrated to experience this negative effect (zeolites appears to be more sensible to water presence). Few studies really dealt with this issue in detail when analyzing the suitability of CO_2 capture

through PSA processes. Some experimental studies have been conducted both with zeolites [48-50] and with activated carbons [36, 51, 52]. However, not much has been done regarding modeling. This can be considered as a big gap, especially when considering post-combustion application where significant amount of water is present in the flue gas. The common approach suggested in the literature is to remove water prior the CO_2 capture unit by means of a separate PSA unit or a pre-layer of selective adsorbents like activated alumina or silica gel desiccants [16, 53]. These methods have to prove to perform satisfactorily integrated in the complex arrangement of a power plant with CO_2 capture systems. Further, they will result in additional power consumption.

In the post-combustion simulation proposed, water is removed to as large extent as possible by condensation, and the remaining water is neglected in the PSA process due to lack of modeling data. The effect of this approximation could not be evaluated and would need to be investigated. For pre-combustion applications the content of water in the syngas entering the PSA unit is down to trace level (0.03%). As long as a more efficient regeneration procedure (e.g., heating of the bed) is planned after a certain number of cycles, in order to avoid water accumulation, the performance should not be significantly affected [7]. Thus, the water content was neglected in the present work without further concerns.

3.4. Solution of the PSA model

The described modeling framework for the PSA process results in a set of partial differential and algebraic equations (PDAEs). The solution was obtained implementing the modeling equations in gPROMS environment (Process System Enterprise, London, UK). The set of PDAEs requires a considerable computational effort in order to be solved. One way to simplify the model, thus to reduce the computational time, was to adopt a one-column approach. This modeling strategy consists in simulating just one of the columns of the whole train [7, 25, 54, 55]. The interactions between different columns are accounted for by virtual gas streams which are defined through the information stored in the previous cycles. The rinse, purge and pressure equalization-pressurization steps rely on this modeling technique. Adopting this simplification, it is essential to assure that the mass balances are always closed. This is rather straightforward for the rinse and purge steps, while the pressure equalization steps requires an additional effort. In fact, an appropriate value of the equalization pressure needs to be set, in order to avoid inconsistency in the mass balances. The procedure outlined by Casas et al. [25] was applied to determine this pressure level.

The discretization algorithm applied for the numerical solution of the model is the Centered Finite Difference Method (CFDM). The spatial domain was discretized in 150 intervals. A higher number of discretization points was not used, because it would have significantly increased the computational time, without increasing in a similar manner the accuracy of the simulation.

The columns are considered to be initially filled with nitrogen and hydrogen, respectively in the post and pre-combustion scenario. The simulation is stopped when the Cycle Steady State (CSS) arises. At CSS the process repeats itself invariably, meaning that the conditions at the end of each cycle are the same as those at the beginning. Whilst the operation of a single column remains batchwise, the process reaches a steady condition. All the results presented refer to the cycles at CSS.

4. Results and discussion

4.1. Definition of the performance parameters

The CO_2 separation performance is primarily evaluated in terms of CO_2 recovery (R_{CO2}) and purity (P_{CO2}). In the pre-combustion scenario it is also useful to define the H_2 recovery (R_{H2}), giving that H_2 is fuelling the downstream gas turbine cycle. The CO_2 recovery may be misleading when large energy penalties result from the CO_2 separation process. For this reason, an additional parameter was introduced, namely the CO_2 capture efficiency (η_{CO2}). The CO_2 capture efficiency is the real measure to what extent the CO_2 is captured from a power plant, relatively to a reference plant without CO_2 capture. The aforementioned parameters are defined as following:

$$R_{CO_2} = \frac{\dot{m} \text{ of } CO_2 \text{ in the product stream}}{\dot{m} \text{ of } CO_2 \text{ formed}} \tag{10}$$

$$P_{CO_2} = CO_2 \text{ volumetric concentration in the product stream} \tag{11}$$

$$R_{H_2} = \frac{\dot{m} \text{ of } H_2 \text{ entering the gas turbine as fuel}}{\dot{m} \text{ of } H_2 \text{ entering the } CO_2 \text{ separation unit}} \tag{12}$$

$$\eta_{CO_2} = 1 - \frac{\eta_{net} \text{ for the reference plant without } CO_2 \text{ capture}}{\eta_{net} \text{ for the plant implementing } CO_2 \text{ capture}} \left(1 - R_{CO_2}\right) \tag{13}$$

The energy efficiency of the plant is evaluated through the net electric efficiency (η_{net}), referred to the LHV:

$$\eta_{net} = \frac{\text{Net electrical output}}{\text{Net fuel input}} \tag{14}$$

The footprint of the CO_2 separation technology is evaluated in terms of square meters occupied by the relative unit. The preliminary analysis carried out considers the size and the number of columns necessary for the CO_2 separation process. A more thorough analysis, including all the equipment relative to the separation process, would be needed in order to obtain more reliable outputs. However, it has been considered beyond the sake of the present work, which aims to give a first assessment on the possible dimensions of the units and on the difference between the separation techniques.

4.2. Post-combustion PSA process

Liu et al. [16] demonstrated that, in order to achieve the requested performance in terms of CO_2 recovery and purity, the flue gas resulting from the combustion of coal needs to undergo a two-stage PSA process. The first stage considered in the current work consists in a three-bed and five-step cycle (**Figure 4**). Since no flue gas compression is implemented upstream the PSA unit, the flue gas enters at about atmospheric pressure. The aim of the first stage is to achieve the highest possible CO_2 recovery. As a tradeoff, it is not possible to achieve very high CO_2 purity. The regeneration process is carried out by decreasing the pressure to 0.1 bar. This pressure value has been suggested in many studies [14, 16, 18, 19, 23]. The regeneration pressure to be applied is dependent on the shape of the adsorbent isotherm and on the degree of vacuum to reach in order to guarantee proper bed regeneration. 0.1 bar seemed to balance the different requirements. Other values may have been considered but the advantages in terms of energy savings obtained with a higher regeneration pressure are counterbalanced by lower separation performance. The other way around with lower regeneration process. As an example, some simulations were implemented with the vacuum level set to 0.2 bar. Whilst the energy penalty could be effectively reduced of about 0.5%, the overall CO_2 recovery dropped under the target value (86.8 %). The CO_2 enriched-gas leaving from the blowdown and purge steps are then collected and sent to the second PSA stage, a two-bed five-step cycle (two-bed six-step if purge is implemented), where it is further purified. In order to enhance the second PSA process performance, a compression of the gas stream is implemented between the PSA stages. The gas is brought up to 2 bar before undergoing the second adsorption process. **Figure 6** shows the overall levels of CO_2 recovery and CO_2 purity obtained in the PSA process (after the two PSA stages) by varying the Purge-to-Feed mole flow rate ratio (P/F) of the second PSA stage. It is clear from the figure that there is a tradeoff between CO_2 recovery and purity. The highlighted point in **Figure 6** (P_{CO2} = 95.1% and R_{CO2} = 90.2%) represents the PSA operating conditions selected for the process to be matched with the power plant. It refers to a PSA process in which the purge step has not been implemented, hence with a P/F ratio equal to zero. This configuration was

chosen because it is able to contemporary fulfill the specification of CO_2 recovery and purity. Additionally, the absence of a purge step simplifies the process configuration. The resultant characteristics of the two PSA stages, which were selected to be integrated in the ASC plant, are reported in **Table 4**.

The PSA columns were initially sized in order to be able to process the entire flow rate. Since an excessively large diameter would have been required, a maximum size of 8 m was stated. A limitation to the superficial velocity was also introduced (0.15 m/s), in order to maintain the pressure drop in the column within a certain threshold (≈ 0.1 bar). The superficial velocity adopted was also verified to be lower than the minimum fluidization velocity. These design considerations implied the need for splitting the total flow rate in a number of trains, respectively 73 and 23 for the first and second PSA stage. Fewer trains are needed in the second PSA stage because large part of the undesired components has already been separated in the first PSA stage.

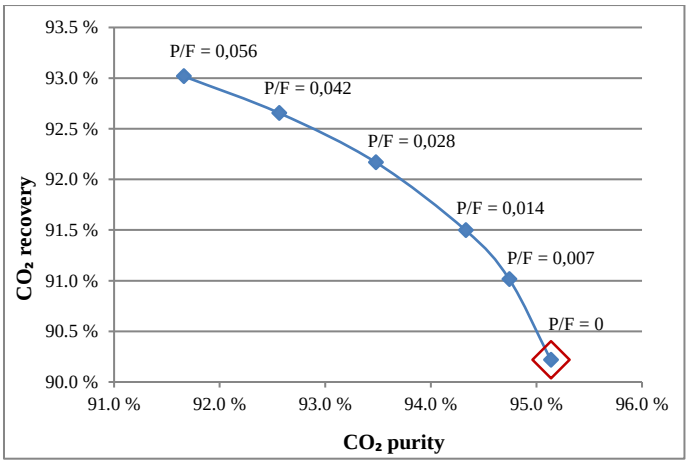

Figure 6. CO_2 separation performance of the PSA process in the post-combustion scenario. Results reported refer to different Purge-to-Feed ratio (P/F) of the mole flow rates in the second PSA stage.

Table 4. Scheduling, characteristics and performance of the PSA process in the post-combustion scenario.

	Step time (s)							Mole flow rate (mol/s)			CO_2	
Stage	**F**	**R**	**D**	**BD**	**Pu**	**P**	**FP**	**Feed**	**Purge**	**Rinse**	**Purity**	**Recovery**
1	702	234	0	702	234	-	234	304,3	91,3	91,3	49,7 %	93,8 %
2	650	-	50	830	-	50	180	360,0	-	-	95,1 %	96,1 %

4.3. Post-combustion scenario analysis

Table 5 summarizes the outcome of the full-plant analysis carried out on the three cases considered for the post-combustion scenario. The plant without CO_2 capture facilities and the plant with a state-of-the-art absorption unit were defined in compliance with the framework determined in the EBTF project [33]. They are meant to be the basis for comparison with the ASC plant integrated with PSA, defined in this work. All the simulations were carried out with the same net fuel input.

Separation performance. The CO_2 separation performance of the PSA process succeeds to meet the required specifications (R_{CO2} = 90.2% and P_{CO2} = 95.1%). If necessary, those values can be further increased at the expense of a higher energy consumption. As an example, a flue gas compression can be implemented before the PSA unit. The resulting increase in the flue gas total pressure would imply an increase of the CO_2 partial pressure, positively affecting the adsorption process. A simulation was run to evaluate this option, considering a flue gas compression from 1 bar to 1.5 bar. The outputs fully met the CO_2-rich stream specifications (R_{CO2} = 90.85% and P_{CO2} = 95.42%) even applying a lower pressure at the entrance of the second PSA unit (i.e., 1.5 bar instead of 2 bar). However, the compression of the flue gas would be an energy demanding process and the impact on the energy balance of the system is evaluated later. The general outcome is that the CO_2 separation performance of the PSA unit, defined

including two following PSA stages, is able to reach the target levels of CO_2 recovery and purity, and to return a CO_2 efficiency even slightly higher than absorption. Moreover, by playing with the PSA process configuration, it is possible to further raise or lower down the separation performance with a consistent impact on the energy penalty: the highest the desired separation performance, the highest is the expected energy penalty.

Energy performance. PSA demonstrates to be competitive with absorption when looking at the energy analysis. The attained net electrical efficiency is slightly higher to that associated with the absorption-based plant. The reference ASC plant without CO_2 capture displayed a η_{net} of 45.1%. It drops to 34.2% and 34.8%, respectively with CO_2 capture by absorption and PSA. Before it was mentioned the possibility of carrying out a flue gas compression (up to 1.5 bar) upstream the PSA process, attaining enhanced CO_2 separation performance. The energy spent for the compression would have a significant impact on the energy balance of the plant, lowering the final η_{net} down to 33.6%. A reason that may justify such a procedure is the benefit that would be obtained in terms of sizes and footprint of the separation unit. Thus, the possibility will be still mentioned in the footprint section, but, otherwise, this option does not appear to be worth of further analyses. The most significant power consumptions, contributing to reduce the η_{net} of the plant in the presence of CO_2 capture processes, are shown in **Figure 7**. It is worthwhile to mention that, in order to be able to compare the difference sources of power losses, the power consumption connected to steam extractions needs to be defined (while all the others are direct electric power consumptions). In fact, the reduction in power output is less than the heat content of the steam. It was evaluated considering the missing expansion of the steam between the extraction point and the downstream condenser, the steam condition at the extraction point and the steam turbine efficiency. Equation (15) shows the methodology adopted:

$$Power\ consumption\ due\ to\ steam\ extraction = \eta_{is,st}\dot{m}_{steam}c_p T_1\left[1-\left(\frac{P_2}{P_1}\right)^{\frac{\gamma-1}{\gamma}}\right] \quad (15)$$

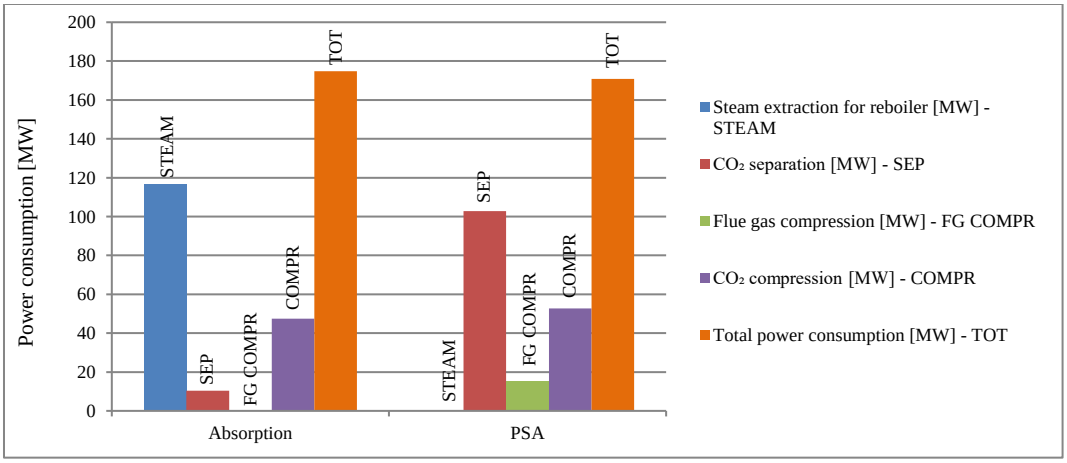

Figure 7. Power consumptions related to the CO_2 capture and compression process for the post-combustion scenario.

The total power consumption is slightly lower for the PSA case, as was easily predictable given the higher η_{net}. When applying an absorption process for capturing CO_2, the largest share of power consumption is connected to the reboiler heating duty for the regeneration of the solvent. In order to comply with this energy demand, steam is extracted from the turbine. This procedure results in a decrease of the gross power output of the plant of about 113.6 MW. The other significant power consumption is related to the compression of the CO_2-rich stream. A five-stage intercooled compressor is used to raise the pressure from 1.7 bar to 110 bar for transport (47.5 MW). In the PSA case the process is not demanding for any steam extraction. However, other sources of power consumptions are present. They are related to the pressure modifications undergone by the flue gas, necessary to carry out the adsorption-desorption process. The term defined as CO_2 separation power consumption includes in the PSA case:

the power requested by the vacuum pumps to establish the vacuum for the regeneration of the bed (95.5 MW); the power supplied to the fan to overcome the pressure drops during the feed, feed pressurization and rinse step (7.3 MW). The CO_2 separation power consumption results to be the largest source of power loss (102.8 MW), while in the absorption case it has a limited impact (10.4 MW mainly due to the consumption of the pumps for the solvent circulation). The flue gas compression occurring between the two PSA stages has a non-negligible impact on the energy balance, accounting for 15.4 MW. In the PSA case the CO_2-rich stream compression displays a power consumption of 52.8 MW. The compression power duty is larger than in the absorption case mainly because of the highest pressure ratio to provide. The CO_2-rich stream leaves the PSA process at a lower pressure level (1 bar) compared to that resulting from the absorption process (1.7 bar). In conclusion, capturing CO_2 in a PSA process displays the big advantage of not requiring any steam, leaving untouched the steam turbine cycle. The implementation of a PSA process introduces new sources of power consumptions connected to the pressure swing processes necessary to comply with the requested CO_2 separation performance. However, the overall balance seems positive under an energy point of view. It is worth to mention that the pumps and compressors simulated have been considered to operate at steady state. This is a strong simplification given the inherent dynamic behavior of a PSA process. It is not known to what extent a discontinuous feed to those devices can negatively affect their performance.

Table 5. Main outputs of the full-plant analysis in the post-combustion scenario.

Plant summary	**No Capture**	**Absorption**	**PSA**
Power inputs			
Coal flow rate [kg/s]	66,2	66,2	66,2
Coal LHV [MJ/kg]	25,2	25,2	25,2
Net fuel input [MW_{th}]	1665,5	1665,5	1665,6
Power outputs			
Steam turbine output [MW]	828,1	714,6	827,3
Gross electric output [MW]	828,1	714,6	827,3
CO_2 separation power consumption [MW]	-	10,4	102,8
Flue gas compression power consumption [MW]	-	0,0	15,4
CO_2 compression power consumption [MW]	-	47,5	52,8
Miscellaneous auxiliaries [MW]	77,4	87,0	77,5
Total auxillary power consumption [MW]	77,4	144,8	248,4
Net electrical output [MW]	750,7	569,7	578,9
Plant performance			
Net electric efficiency [%]	45,1 %	34,2 %	34,8 %
CO_2 purity [%]	-	100,0 %	95,1 %
CO_2 recovery [%]	-	90,0 %	90,2 %
CO_2 capture efficiency [%]	-	86,8 %	87,3 %

Footprint. The mole flow rate entering a single PSA train cannot be further increased, compared to the level reported in **Table 4**, for limitations related to the pressure drop and the minimum fluidization velocity. Treating the total flue gas volume, the plant needs a large number of PSA trains (i.e., about 73 and 23 trains for the first and second PSA stage). Each PSA train is constituted by 3 and 2 columns, respectively in the first and second PSA

stage, and the diameter of a column was set to 8 m. **Table 6** shows an estimation of the footprints of the two separation techniques considered. The absorption column diameter was calculated by defining a reasonable superficial velocity of the flue gas entering the column (i.e., 2 m/s). It becomes clear that the total footprint of the CO_2 capture unit is excessive to be considered feasible. A way to partially reduce the footprint could be to introduce a flue gas compression before the PSA unit. Compressing the flue gas up to 1.5 bar demonstrated to lead to a reduction in the number of necessary PSA trains of about 9 units. It was already verified that this operation would also be beneficial for the CO_2 separation process. However, the final footprint would still be much larger than that of the absorption-counterpart. Not to mention the additional power consumption introduced which would severely affect the process competitiveness under an energy efficiency point of view.

Table 6. Footprint analysis for the post-combustion scenario.

	Absorption	PSA
Column diameter (m)	20,7	8,0
Number of columns	2	264
Footprint (m^2)	674	13285

4.4. Pre-combustion PSA process

The PSA process is supposed to be able to process the syngas and return two streams: a CO_2-rich stream to be sent to compression and transportation; and a CO_2-lean stream, rich in H_2, to be fed to the gas turbine as fuel. Both streams request some purity characteristics to be fulfilled, namely CO_2 and/or H_2 purity and recovery. Previous studies [25] suggested that a single PSA stage would have been able to fulfill these requirements in conditions typical for a pre-combustion application. However, Casas et al. [25] simulated a gas stream which contains only H_2 and CO_2. When applying a realistic syngas composition, the results of the simulations became different from those expected. The PSA layout adopted in the present work is a seven-bed and twelve-step cycle and the regeneration pressure was set to 1 bar. Some demonstrative simulations were run to assess the effectiveness of the selected regeneration process. Higher regeneration pressure levels can bring an improvement on an energy point of view, although the reduced purity could partially even out the expected reduction in compression power consumption. Conversely, the separation performance decreases according to the less effective regeneration process. 1 bar appeared to be the regeneration pressure which was closer to meet both separation and energy specifications. **Figure 8** shows the levels of CO_2 recovery and CO_2 purity obtained in the assessed PSA process by varying the Purge-to-Feed mole flow rate ratio (P/F). The values reported in the figure refer only to the PSA unit. The overall plant CO_2 purity and recovery will be different since an additional flash separation process is implemented after the PSA process. **Figure 8** makes clear that the PSA process is not quite able to match the specifications. Whilst the CO_2 recovery can be pushed easily over the target value of 90%, the CO_2 purity hardly reaches values around 85%. A further increase of the CO_2 purity appears difficult to achieve and would come at the expense of the CO_2 recovery, which would drastically decrease. Realizing the impossibility to reach the desired output streams characteristics within the PSA unit, the strategy was modified. A solution could have been to introduce an additional PSA stage (likewise post-combustion scenario) or better to apply a dual PSA process [56]. Considerations mainly regarding the possible footprint related to a second PSA train lead us to choose a different option. Nevertheless, the dual PSA process could result competitive and should be matter of further investigations. To comply with the selected alternative, the CO_2 recovery target was set to the highest possible level, while a relatively lower value of CO_2 purity was accepted. It was then introduced a further CO_2 purification process downstream of the PSA unit. It consists of a double flash separation integrated in the CO_2 compression process (**Figure 3**). Referring to Posch and Haider [35], the temperatures selected at the outlet of each heat exchanger were set respectively to -30°C and -54.5°C. The gas stream is compressed up to 30 bar before entering the flash separation unit. Implementing this additional separation step, the final result in terms of CO_2 purity (P_{CO2}=98.9%) and recovery (R_{CO2}=89.8%) basically fulfilled the requirements. The H_2 recovery (R_{H2}=99.6%) was satisfactory as well. The operating conditions selected for the full-plant analysis are those represented by the highlighted point in **Figure 8** (i.e., P/F = 0.140). This configuration was chosen because it provides a good balance between separation and energy performances. **Table 7** displays the relative PSA characteristics, together with the separation

performance obtained. The overall separation performance, resulting from the integration of the flash separation unit, is also reported.

The criteria adopted for the design of the pre-combustion PSA unit are similar to those discussed in the post-combustion scenario. A less stringent limitation was imposed to the maximum pressure drop (≈ 0.15 bar) and a lower superficial velocity had to be utilized (0.08 m/s) in order to make up for the higher operating pressure (as can be inferred from the Ergun equation, the higher the operating pressure, the larger the pressure drop). However, a single PSA train was evaluated as able to process the entire syngas flow rate. Accordingly, the columns diameter was set to 6.6 m.

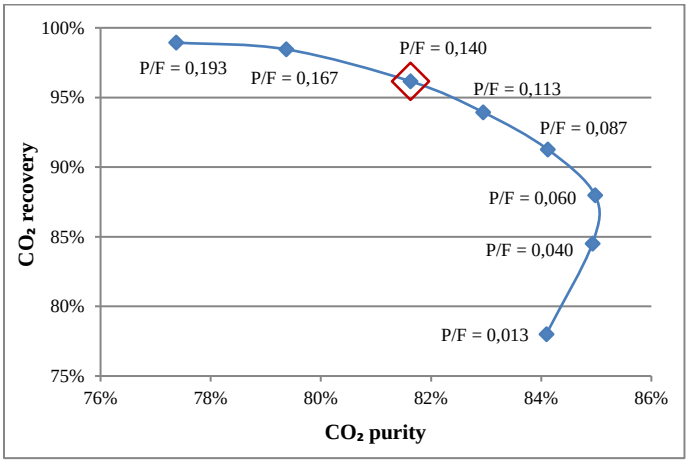

Figure 8. CO_2 separation performance of the PSA process in the pre-combustion scenario. Results reported refer to different Purge-to-Feed ratio (P/F) of the mole flow rates.

Table 7. Scheduling, characteristics and performance of the PSA process in the pre-combustion scenario

	Step time (s)							Mole flow rate (mol/s)		CO_2	
	F	**D X 4**	**BD**	**Pu**	**P X 4**	**N X 4**	**FP**	**Feed**	**Purge**	**Purity**	**Recovery**
PSA	90	41	80	59	41	8	41	3771,6	525,0	81,6 %	96,2 %
PSA + flash	-	-	-	-	-	-	-	-	-	98,9 %	89,8 %

4.5. Pre-combustion scenario analysis

Table 8 summarizes the outcome of the full-plant analysis carried out on the three cases considered for the pre-combustion scenario. The plant without CO_2 capture facilities and the plant with a state-of-the-art absorption unit were defined in compliance with the framework determined in the EBTF project [33]. They are meant to be the basis for comparison with the IGCC plant integrated with PSA, defined in this work. The simulations were run such as to obtain similar exhaust gas flow rates at the gas turbine outlet. This assumption meant to support following comparisons of the results by allowing same size gas turbines to be used for the simulations. The typology of gas turbine considered is large-scale "F class" 50 Hz.

Separation performance. When evaluating the CO_2 separation performance, PSA and double flash process seems to match the requirements. The P_{CO2} is above 95% and R_{CO2} is slightly lower than the target, with a value of 89.8% (at least when considering the CO_2 recovery only for the separation technology**)**. It is important to achieve a high value of P_{CO2} (98.9%), because this is strictly related to the H_2 recovery, which is, in fact, very high as well (R_{H2} = 99.6%). Recovering large part of H_2 is essential in order to guarantee good energy performance of the system. However, the syngas fuelling the gas turbine contains traces of CO and CH_4, products of the gasification process. Their combustion results in the formation of additional CO_2 which has to be taken into account in the CO_2 balance of the overall plant. For this reason, there is an additional CO_2 recovery parameter, which is considering the total CO_2 formed. The R_{CO2} for the PSA case drops then to 86.1% which is not fully fulfilling the requirement.

Conversely, absorption as decarbonization technique succeeds to reach the suggested target values, attaining P_{CO2}, overall R_{CO2} and R_{H2} of 100%, 90.5% and 100% respectively. The CO_2 capture efficiency well summarizes the discussed picture. η_{CO2} for the PSA-based plant is 81.8%, a value that can be considered acceptable, although lower than that achieved with absorption (88.1%).

Energy performance. The energy analysis of the pre-combustion scenario reveals that absorption is not clearly outperforming PSA. The reference IGCC plant without CO_2 capture attains a η_{net} of 47.3%. Introducing an absorption unit or a PSA unit for CO_2 capture drops the η_{net} down to 37.1% and 36.2% respectively. The difference between the two cases is rather small (0.9%). A breakdown analysis of the power consumption, related to the integration of a CO_2 capture unit, highlights some differences (see **Figure 9**). Since some power consumptions are characteristic of a pre-combustion application, they are described hereafter (the calculation of the equivalent power consumption is also explained, if the term reported is not a direct electric power consumption):

- WGS LHV reduction: the WGS process produces a reduction of the syngas LHV (partially balanced by a higher mass flow rate). The reduction in the fuel energy is converted into power consumption by considering the net efficiency of the plant.
- LHV lost in CO_2 separation: since traces of hydrogen and carbon monoxide are leaving with the CO_2-rich stream, their heating value is wasted. The reduction in the fuel energy is converted into power consumption considering the net efficiency of the plant.
- Steam extraction for WGS: some steam need to be extracted by the steam turbine in order to be fed to the WGS process. The missing expansion of that steam causes a reduction in the steam turbine power output. The power consumption is calculated as described in the post-combustion scenario for steam extractions.

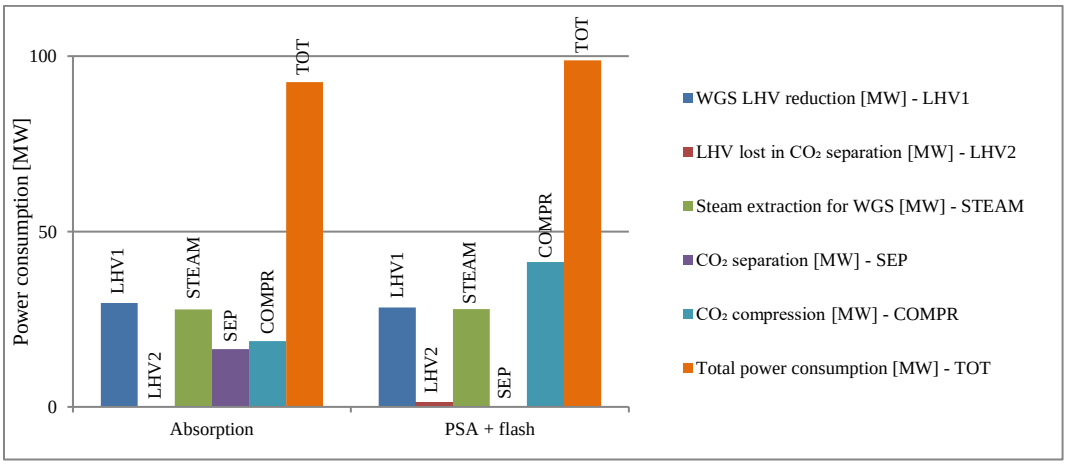

Figure 9. Power consumptions related to the CO_2 capture and compression process for the pre-combustion scenario

The PSA unit does not directly require much energy. The CO_2 separation power consumption is very small (≈ 0.05 MW) and mainly due to the fans for overcoming the pressure drop in the bed. Since the regeneration pressure is atmospheric, no vacuum pumps need to be installed. The avoidance of a rinse step in the PSA process configuration is also contributing to limit the power consumption. In the absorption case the CO_2 separation power consumption is larger. The required 16.5 MW are mostly supplied to the pumps for the solvent circulation. However, the particular configuration of the absorption/regeneration process is favorable when considering the power for the compression of the CO_2-rich stream. The regeneration process for the absorption case is occurring at three different pressure levels (12.7, 7.5 and 1.1 bar). In the PSA process the CO_2-rich stream leaves the unit at 1 bar, meaning that the pressure ratio that the compressor has to provide is, on average, larger. Moreover, in the double flash separation process, the CO_2-rich streams leaving the flashes are partially expanded in adiabatic throttles, since by entering counter-currently the heat exchangers they assure the necessary cooling potential. Hence, the CO_2 compression duty is further increased. The CO_2 compression power consumption results to be 41.3 MW for the PSA case, while for the absorption case is 18.7 MW. It can be argued that the power saved in the separation process, adopting PSA, is more than balanced by the additional power demand for CO_2 compression.

The other power consumptions evaluated are very similar in both cases, so they do not modify the picture outlined. Summing up, the CO_2 capture through a PSA unit shifts the power consumption from the capture process to the CO_2 compression, while all the other power loss contributions remain almost unchanged. However, the increase in the compression power results to prevail. Accordingly the energy efficiency penalty relative to the PSA case is slightly higher than that relative to the absorption case.

Table 8. Main outputs of the full-plant analysis in the pre-combustion scenario.

Plant summary	No Capture	Absorption	PSA + flash
Power inputs			
Coal flow rate [kg/s]	33,3	38,5	38,5
Coal LHV [MJ/kg]	25,2	25,2	25,2
Net fuel input [MW_{th}]	837,3	968,1	968,2
Power outputs			
Gas turbine output [MW]	253,1	287,9	287,1
Steam turbine output [MW]	192,6	167,6	167,4
Air expander output [MW]	4,5	5,7	5,4
Gross electric output [MW]	450,2	461,1	459,9
CO_2 separation power consumption [MW]	-	16,5	0,0
CO_2 compression power consumption [MW]	-	18,7	41,3
ASU power consumption [MW]	38,9	51,5	51,6
Miscellaneous auxiliaries [MW]	15,5	16,3	16,7
Total auxillary power consumption [MW]	54,3	103,0	109,6
Net electric output [MW]	395,8	358,1	350,2
Plant performance			
Net electric efficiency [%]	47,3 %	37,1 %	36,2 %
CO_2 purity [%]	-	100,0 %	98,9 %
CO_2 recovery - separation technology [%]	-	94,6 %	89,8 %
CO_2 recovery - overall plant [%]	-	90,6 %	86,1 %
H_2 recovery [%]	-	100,0 %	99,6 %
CO_2 capture efficiency [%]	-	88,1 %	81,8 %

Footprint. Given the high pressure at which the syngas enters the PSA unit (38.8 bar), resulting in a relatively low volumetric flow rate, it was possible to design the PSA unit in a way that all the syngas is processed by a single PSA train. The superficial velocity adopted is able to maintain the pressure drop within acceptable limits (≈ 0.15 bar). The value was also verified not to overpass the minimum fluidization velocity at the operating conditions considered. Established the velocity and knowing the volumetric flow rate, the cross sectional area was evaluated and, hence, the diameter of the column. It resulted to be 6.6 m. Even though a PSA train is formed by 7 columns working in parallel, the footprint of the PSA unit appears to be acceptable. However, the footprint of an absorption unit would be much smaller. **Table 9** compares the estimations of the two footprints, highlighting the remarks of

the analysis. The absorption column diameter was calculated by defining a reasonable superficial velocity of the flue gas entering the column (i.e., 1 m/s).

Table 9. Footprint analysis for the pre-combustion scenario

	Absorption	PSA
Column diameter (m)	2,2	6,6
Number of columns	2	7
Footprint (m²)	8	239

5. Conclusions

In the current work, the suitability of PSA process for CO_2 capture in coal-fired power plants has been assessed. The effectiveness of PSA is evaluated on three different levels: CO_2 separation performance, energy efficiency and footprint of the technology. A post- and a pre-combustion scenario have been considered.

In the post-combustion scenario a PSA process is integrated with an Advanced SuperCritical (ASC) pulverized coal plant. The outputs of the full-plant analysis were compared to those of a similar plant implementing a state-of-the-art absorption process for capturing CO_2. A two stage PSA process is necessary in order to achieve satisfactory characteristics of the CO_2-rich stream to be transported and stored. The first PSA stage is a three-bed five-step cycle, the second is a two-bed five-step cycle. The resulting CO_2 purity (P_{CO2} = 95.1%) and recovery (R_{CO2} = 90.2%) fulfill the target levels established (i.e., $P_{CO2} \approx 95\%$ and $R_{CO2} \approx 90\%$). The utilization of a PSA process shifts the power consumption related to CO_2 capture from a thermal duty for regenerating the solvent (i.e., amine absorption) to direct electrical power for vacuum pumps and compressors. The resultant energy penalty is competitive with that of the benchmark absorption-based plant, as it was possible to obtain a net electrical efficiency slightly higher. The main obstacle for the suitability of PSA in post-combustion application is related to its footprint. The flue gas flow rate has to be split in a large number of PSA trains (about 73 and 23 for first and second PSA stage) to be processed. Given the diameter (8 m) of each of the columns constituting a train, the footprint of the PSA unit is much larger compared to the reference absorption unit. Modifications in the process configuration may bring an improvement in this sense, at the expense of other performance indicators. However, the gap is so large that is difficult to imagine filling it within the considered process framework.

The application of a PSA process in a pre-combustion scenario returns promising results. The PSA process is integrated in an Integrated Gasification Combined Cycle (IGCC) plant. The outputs of the full-plant analysis were compared to those of a similar plant implementing a state-of-the-art absorption process for capturing CO_2. The PSA process considered was a seven-bed and twelve-step cycle. In order to comply with the separation performance specifications, an additional double flash separation process was integrated in the CO_2 compression unit. The obtained purity (P_{CO2} = 98.9 %) of the CO_2-rich stream fulfills the requirement. The overall CO_2 recovery (R_{CO2} = 86.1 %) is slightly lower compared to the level aimed (i.e., 90%). However, a rearrangement of the process could be able to trade off part of the purity for a higher recovery, so that the process meets both the requirements. The absorption process fully complies with the target values. The energy analysis of the simulated PSA-based plant yields a η_{net} of 36.2%. The η_{net} of the reference IGCC plant without CO_2 capture is 47.3%, while integrating an absorption process for CO_2 capture drops it to 37.1%. The difference of energy efficiency between the two cases studied is lower than 1%. The footprint of the PSA unit is not problematic, since a single PSA train (7 columns of 6.6 m diameter) is able to process the volumetric flow rate of syngas. In conclusion, PSA process has the chance to become competitive in a pre-combustion scenario for CO_2 capture. The general performance obtained is slightly lower compared to that relative to a plant implementing an absorption process. On the other hand, PSA is a less mature technology for CO_2 capture applications. Therefore, substantial improvements are likely achievable. For instance, the layout of the whole process may be further optimized. Advancements in material technology may also introduce adsorbents with increased uptake capacity and selectivity, and possibly with higher thermal resistance. Such an accomplishment would make possible better separation performance and a higher degree of process integration. Hence, there is reason to believe that PSA can become a suitable alternative to absorption for pre-combustion CO_2 capture.

Acknowledgements

The authors gratefully acknowledge the financial support provided through the "EnPe – NORAD's Programme within the energy and petroleum sector".

Nomenclature

a_i	number of neighboring sites occupied by adsorbate molecule for species i
C_i	gas concentration of species i, mol/m^3
C_p	specific heat at constant pressure, MJ/(kg · K)
$C_{p,ads}$	adsorbed phase specific heat at constant pressure, J/(kg · K)
$C_{p,g}$	gas specific heat at constant pressure, J/(mol · K)
$C_{p,s}$	particle specific heat at constant pressure, J/(kg · K)
C_{tot}	total gas concentration, mol/m^3
$D_{ax,i}$	axial dispersion coefficient of species i, m^2/s
$D_{c,i}$	micropore diffusivity of species i, m^2/s
$D_{0c,i}$	limiting micropore diffusivity at infinite temperature of species i, m^2/s
$D_{mg,i}$	multicomponent diffusion coefficient of species i, m^2/s
$D_{g,ii'}$	binary diffusion coefficient of the ij system, m^2/s
d_p	particle diameter, m
$E_{a,i}$	activation energy of species i, J/mol
$\Delta H_{r,i}$	heat of adsorption of species i, J/mol
k_f	gas conductivity, J/(s · m · K)
k_i	equilibrium constant of species i, Pa^{-1}
$k_{\infty,i}$	adsorption constant at infinite temperature of species i, Pa^{-1}
$k_{LDF,i}$	linear driving force coefficient, s^{-1}
$\dot{m}$	mass flow rate, kg/s
$\dot{n}$	mole flow rate, mol/s
P	pressure, Pa
P_{CO2}	CO_2 purity
Pr	Prandtl number
q_i^*	equilibrium adsorbed concentration of species i, mol/kg
$\overline{q}_i$	averaged adsorbed concentration of species i, mol/kg
$q_{m,i}$	specific saturation adsorption capacity of species i, mol/kg
R	universal gas constant, Pa · m^3/(mol · K)
R_{CO2}	CO_2 recovery
R_{H2}	H_2 recovery
Re	Reynolds number
r_c	crystal radius, m
T	temperature, K
u_s	superficial velocity, m/s
y_i	mole fraction of species i
z	axial direction, m

Greek letters

γ	specific heat ratio
ε	bed porosity
ε_p	particle porosity
η_{CO2}	CO2 capture efficiency
η_{is}	isentropic efficiency
η_{net}	net electric efficiency
λ_{ax}	axial thermal dispersion coefficient, J/(s · m · K)
μ	dynamic viscosity, Pa · s

ξ_i	diffusion parameter for species i
ρ_g	gas volumetric mass density, kg/m3
ρ_p	volumetric mass density of the particle, kg/m^3
χ_{LDF}	linear driving force geometrical factor (15 for zeolite 5A, 3 for activated carbon)

Acronyms

ASC	advanced supercritical
C	compressor
CCS	carbon capture and storage
DHU	dehydration unit
FS	flash separator
IC	inter-cooler
IGCC	integrated gasification combined cycle
LHV	lower heating value
LDF	linear driving force
MSHE	multi stream heat exchanger
PSA	pressure swing adsorption
TV	throttling valve
WGS	water gas shift

Subscripts

i	species

Superscripts

NC	number of components

Appendix A. Calculation of the transport parameters.

Table 1. Transport parameters equations.

Axial dispersion [57]

$$D_{ax,i} = \left(0.45 + 0.55\varepsilon\right) D_{g,i}^{m} + 0.35 \frac{d_p}{2} \left|u_s\right| \tag{16}$$

Wilke model for a single-phase mixture of gases [58, 59]

$$D_{g,i}^{\mathrm{m}} = \frac{1 - y_i}{\sum_{i' \neq i} \frac{y_{i'}}{D_{\mathrm{g},ii'}}} \tag{17}$$

$$D_{\mathrm{g},ii'} = \frac{10^{-3} T_{\mathrm{g}}^{1.75} \left[\frac{1}{M_i} + \frac{1}{M_{i'}}\right]^{1/2}}{(p_{\mathrm{g}} / 101325)\left[\left(\sum_i \xi_i\right)^{1/3} + \left(\sum_{i'} \xi_{i'}\right)^{1/3}\right]^2} \tag{18}$$

Micropore diffusivity [57]

$$\frac{D_{c,i}}{r_c^2} = \frac{D_{c,i}^0}{r_c^2} \exp\left(-\frac{E_{a,i}}{RT}\right) \tag{19}$$

Axial thermal dispersion coefficient [60]

$$\frac{\lambda_{ax}}{k_f} = 7 + 0.5 \,\mathrm{Pr}\,\mathrm{Re} \tag{20}$$

Appendix B. Boundary conditions for the PSA processes.

Table 2. Boundary conditions adopted for the PSA processes. The co-current blowdown and co-current pressure equalization boundary conditions are the same as the counter-current counterpart applied inverted at the extremities of the column.

Feed: z = 0

$$\varepsilon D_{ax,i}\frac{\partial C_i}{\partial z} = -u_s\left(C_{F,i} - C_i\right)$$

$$\dot{n} = \dot{n}_F$$

$$\lambda_{ax}\frac{\partial T}{\partial z} = -u_s C_p C_{tot}\left(T_F - T\right)$$

z = L

$$\frac{\partial C_i}{\partial z} = 0$$

$$P = P_F$$

$$\frac{\partial T}{\partial z} = 0$$

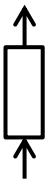

Rinse: z = 0

$$\varepsilon D_{ax,i}\frac{\partial C_i}{\partial z} = -u_s\left(C_{R,i} - C_i\right)$$

$$\dot{n} = \dot{n}_R$$

$$\lambda_{ax}\frac{\partial T}{\partial z} = -u_s C_p C_{tot}\left(T_R - T\right)$$

z = L

$$\frac{\partial C_i}{\partial z} = 0$$

$$P = P_F$$

$$\frac{\partial T}{\partial z} = 0$$

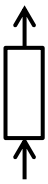

Pressure equalization – depressurization: z = 0

$$\frac{\partial C_i}{\partial z} = 0$$

$$\dot{n} = 0$$

$$\frac{\partial T}{\partial z} = 0$$

z = L

$$\frac{\partial C_i}{\partial z} = 0$$

$$P = P_{eq}$$

$$\frac{\partial T}{\partial z} = 0$$

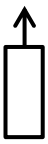

Counter-current blowdown: z = 0

$$\frac{\partial C_i}{\partial z} = 0$$

$$P = P_{BD}$$

$$\frac{\partial T}{\partial z} = 0$$

z = L

$$\frac{\partial C_i}{\partial z} = 0$$

$$\dot{n} = 0$$

$$\frac{\partial T}{\partial z} = 0$$

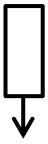

Purge: z = 0

$$\frac{\partial C_i}{\partial z} = 0$$

$$P = P_{BD}$$

$$\frac{\partial T}{\partial z} = 0$$

z = L

$$\varepsilon D_{ax,i}\frac{\partial C_i}{\partial z} = -u_s\left(C_{Pu,i} - C_i\right)$$

$$\dot{n} = \dot{n}_{Pu}$$

$$\lambda_{ax}\frac{\partial T}{\partial z} = -u_s C_p C_{tot}\left(T_{Pu} - T\right)$$

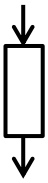

Counter-current pressure equalization – Pressurization: z = 0

$$\frac{\partial C_i}{\partial z} = 0$$

$$\dot{n} = 0$$

$$\frac{\partial T}{\partial z} = 0$$

z = L

$$\varepsilon D_{ax,i}\frac{\partial C_i}{\partial z} = -u_s\left(C_{eq,i} - C_i\right)$$

$$\dot{n} = \dot{n}_{eq}$$

$$\lambda_{ax}\frac{\partial T}{\partial z} = -u_s C_p C_{tot}\left(T_{eq} - T\right)$$

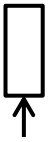

Feed pressurization: z = 0

$$\frac{\partial C_i}{\partial z} = 0$$

$$\dot{n} = 0$$

$$\frac{\partial T}{\partial z} = 0$$

z = L

$$\varepsilon D_{ax,i}\frac{\partial C_i}{\partial z} = -u_s\left(C_{FP,i} - C_i\right)$$

$$P = P_{FP}$$

$$\lambda_{ax}\frac{\partial T}{\partial z} = -u_s C_p C_{tot}\left(T_{FP} - T\right)$$

References

1. IPCC, *Climate Change 2013: The Physical Science Basis Contribution of Working Group I to the Fifth Assessment Report of the Intergovernmental Panel on Climate Change*, T.F. Stocker, D. Qin, G.-K. Plattner, M. Tignor, S.K. Allen , J. Boschung, A. Nauels, Y. Xia, V. Bex and P.M. Midgley, Editor 2013: Cambridge University Press, Cambridge, United Kingdom and New York, NY, USA. p. 1535 pp.
2. IPCC, *IPCC Special Report on Carbon Dioxide Capture and Storage. Prepared by Working Group III of the Intergovernmental Panel on Climate Change*, B. Metz, O. Davidson, H. C. de Corninck, M. Loos, and L.A. Meyer, Editor 2005: Cambridge University Press, Cambridge, United Kingdom and New York, NY, USA. p. 442 pp.
3. Ebner, A.D. and J.A. Ritter, *State-of-the-art Adsorption and Membrane Separation Processes for Carbon Dioxide Production from Carbon Dioxide Emitting Industries.* Separation Science and Technology, 2009. **44**(6): p. 1273-1421.
4. Herzog H, M.J., Hatton A., *Advanced Post-Combustion CO2 Capture*, 2009.
5. Cen, P. and R.T. Yang, *Bulk gas separation by pressure swing adsorption.* Industrial & Engineering Chemistry Fundamentals, 1986. **25**(4): p. 758-767.
6. Ribeiro, A.M., et al., *A parametric study of layered bed PSA for hydrogen purification.* Chemical Engineering Science, 2008. **63**(21): p. 5258-5273.
7. Ribeiro, A.M., et al., *Four beds pressure swing adsorption for hydrogen purification: Case of humid feed and activated carbon beds.* AIChE Journal, 2009. **55**(9): p. 2292-2302.
8. Yang, J. and C.-H. Lee, *Adsorption dynamics of a layered bed PSA for H2 recovery from coke oven gas.* AIChE Journal, 1998. **44**(6): p. 1325-1334.
9. Yang, J., C.-H. Lee, and J.-W. Chang, *Separation of Hydrogen Mixtures by a Two-Bed Pressure Swing Adsorption Process Using Zeolite 5A.* Industrial & Engineering Chemistry Research, 1997. **36**(7): p. 2789-2798.
10. Agarwal, A., L.T. Biegler, and S.E. Zitney, *A superstructure-based optimal synthesis of PSA cycles for post-combustion CO2 capture.* AIChE Journal, 2010. **56**(7): p. 1813-1828.
11. Choi, W.-K., et al., *Optimal operation of the pressure swing adsorption (PSA) process for CO2 recovery.* Korean Journal of Chemical Engineering, 2003. **20**(4): p. 617-623.
12. Chou, C.-T. and C.-Y. Chen, *Carbon dioxide recovery by vacuum swing adsorption.* Separation and Purification Technology, 2004. **39**(1–2): p. 51-65.
13. Ishibashi, M., et al., *Technology for removing carbon dioxide from power plant flue gas by the physical adsorption method.* Energy Conversion and Management, 1996. **37**(6–8): p. 929-933.
14. Kikkinides, E.S., R.T. Yang, and S.H. Cho, *Concentration and recovery of carbon dioxide from flue gas by pressure swing adsorption.* Industrial & Engineering Chemistry Research, 1993. **32**(11): p. 2714-2720.
15. Ko, D., R. Siriwardane, and L.T. Biegler, *Optimization of Pressure Swing Adsorption and Fractionated Vacuum Pressure Swing Adsorption Processes for CO2 Capture.* Industrial & Engineering Chemistry Research, 2005. **44**(21): p. 8084-8094.
16. Liu, Z., et al., *Multi-bed Vacuum Pressure Swing Adsorption for carbon dioxide capture from flue gas.* Separation and Purification Technology, 2011. **81**(3): p. 307-317.
17. Mehrotra, A., A. Ebner, and J. Ritter, *Arithmetic approach for complex PSA cycle scheduling.* Adsorption, 2010. **16**(3): p. 113-126.

18. Na, B.-K., et al., *CO2 Recovery from Flue Gas by PSA Process using Activated Carbon.* Korean Journal of Chemical Engineering, 2001. **18**(2): p. 220-227.
19. Na, B.-K., et al., *Effect of Rinse and Recycle Methods on the Pressure Swing Adsorption Process To Recover CO2 from Power Plant Flue Gas Using Activated Carbon.* Industrial & Engineering Chemistry Research, 2002. **41**(22): p. 5498-5503.
20. Nikolic, D., et al., *Generic Modeling Framework for Gas Separations Using Multibed Pressure Swing Adsorption Processes.* Industrial & Engineering Chemistry Research, 2008. **47**(9): p. 3156-3169.
21. Plaza, M.G., et al., *Post-combustion CO2 capture with a commercial activated carbon: Comparison of different regeneration strategies.* Chemical Engineering Journal, 2010. **163**(1–2): p. 41-47.
22. Reynolds, S.P., A.D. Ebner, and J.A. Ritter, *Stripping PSA Cycles for CO2 Recovery from Flue Gas at High Temperature Using a Hydrotalcite-Like Adsorbent.* Industrial & Engineering Chemistry Research, 2006. **45**(12): p. 4278-4294.
23. Takamura, Y., et al., *Evaluation of dual-bed pressure swing adsorption for CO2 recovery from boiler exhaust gas.* Separation and Purification Technology, 2001. **24**(3): p. 519-528.
24. Tlili, N., G. Grévillot, and C. Vallières, *Carbon dioxide capture and recovery by means of TSA and/or VSA.* International Journal of Greenhouse Gas Control, 2009. **3**(5): p. 519-527.
25. Casas, N., et al., *A parametric study of a PSA process for pre-combustion CO2 capture.* Separation and Purification Technology, 2013. **104**(0): p. 183-192.
26. Schell, J., et al., *Precombustion CO2 Capture by Pressure Swing Adsorption (PSA): Comparison of Laboratory PSA Experiments and Simulations.* Industrial & Engineering Chemistry Research, 2013. **52**(24): p. 8311-8322.
27. *The Future of Coal*, 2007, Massachusetts Institute of Technology.
28. Panowski, M., R. Klainy, and K. Sztelder, *Modelling of CO2 Adsorption from Exhaust Gases*, in *Proceedings of the 20th International Conference on Fluidized Bed Combustion*, G. Yue, et al., Editors. 2010, Springer Berlin Heidelberg. p. 889-894.
29. Ho, M.T., G.W. Allinson, and D.E. Wiley, *Reducing the Cost of CO2 Capture from Flue Gases Using Pressure Swing Adsorption.* Industrial & Engineering Chemistry Research, 2008. **47**(14): p. 4883-4890.
30. Liu, Z. and W.H. Green, *Analysis of Adsorbent-Based Warm CO2 Capture Technology for Integrated Gasification Combined Cycle (IGCC) Power Plants.* Industrial & Engineering Chemistry Research, 2014. **53**(27): p. 11145-11158.
31. Gazzani, M., E. Macchi, and G. Manzolini, *CO2 capture in integrated gasification combined cycle with SEWGS – Part A: Thermodynamic performances.* Fuel, 2013. **105**(0): p. 206-219.
32. Manzolini, G., et al., *Integration of SEWGS for carbon capture in natural gas combined cycle. Part A: Thermodynamic performances.* International Journal of Greenhouse Gas Control, 2011. **5**(2): p. 200-213.
33. *DECARBit: Enabling advanced pre-combustion capture techniques and plants. European best practice guidelines for assessment of CO2 capture technologies*, 2011, European Benchmarking Task Force.
34. Pipitone, G. and O. Bolland, *Power generation with CO2 capture: Technology for CO2 purification.* International Journal of Greenhouse Gas Control, 2009. **3**(5): p. 528-534.
35. Posch, S. and M. Haider, *Optimization of CO2 compression and purification units (CO2CPU) for CCS power plants.* Fuel, 2012. **101**(0): p. 254-263.

36. Lopes, F.V.S., et al., *Adsorption of H2, CO2, CH4, CO, N2 and H2O in Activated Carbon and Zeolite for Hydrogen Production.* Separation Science and Technology, 2009. **44**(5): p. 1045-1073.
37. Ruthven, D.M., L.-K. Lee, and H. Yucel, *Kinetics of non-isothermal sorption in molecular sieve crystals.* AIChE Journal, 1980. **26**(1): p. 16-23.
38. Yucel, H. and D.M. Ruthven, *Diffusion of CO2 in 4A and 5A zeolite crystals.* J Colloid Interface Sci, 1980. **74**(1): p. 186-195.
39. Yang, R.T., *Gas Separation By Adsorption Processes*1997.
40. Azevedo, D.C.S. and A.E. Rodrigues, *Bilinear Driving Force Approximation in the Modeling of a Simulated Moving Bed Using Bidisperse Adsorbents.* Industrial & Engineering Chemistry Research, 1999. **38**(9): p. 3519-3529.
41. Rodrigues, A.r.E. and M.M. Dias, *Linear driving force approximation in cyclic adsorption processes: Simple results from system dynamics based on frequency response analysis.* Chemical Engineering and Processing: Process Intensification, 1998. **37**(6): p. 489-502.
42. Sircar, S. and J.R. Hufton, *Why Does the Linear Driving Force Model for Adsorption Kinetics Work?* Adsorption, 2000. **6**(2): p. 137-147.
43. Froment, G.F., K.B. Bischoff, and J. De Wilde, *Chemical Reactor Analysis and Design, 3rd edition*2010: John Wiley & Sons, Inc.
44. Liu, Z., et al., *Adsorption and Desorption of Carbon Dioxide and Nitrogen on Zeolite 5A.* Separation Science and Technology, 2011. **46**(3): p. 434-451.
45. Siriwardane, R., et al., *Adsorption and desorption of CO2 on solid sorbents.* Journal of Energy & Environmental Research, 2001: p. 19-31.
46. Siriwardane, R.V., et al., *Adsorption of CO2 on Zeolites at Moderate Temperatures.* Energy & Fuels, 2005. **19**(3): p. 1153-1159.
47. Harlick, P.J.E. and F.H. Tezel, *An experimental adsorbent screening study for CO2 removal from N2.* Microporous and Mesoporous Materials, 2004. **76**(1-3): p. 71-79.
48. Brandani, F. and D.M. Ruthven, *The Effect of Water on the Adsorption of CO2 and C3H8 on Type X Zeolites.* Industrial & Engineering Chemistry Research, 2004. **43**(26): p. 8339-8344.
49. Gallei, E. and G. Stumpf, *Infrared spectroscopic studies of the adsorption of carbon dioxide and the coadsorption of carbon dioxide and water on CaY- and NiY-zeolites.* J Colloid Interface Sci, 1976. **55**(2): p. 415-420.
50. Li, G., et al., *Dual mode roll-up effect in multicomponent non-isothermal adsorption processes with multilayered bed packing.* Chemical Engineering Science, 2011. **66**(9): p. 1825-1834.
51. Adams, L.B., et al., *An examination of how exposure to humid air can result in changes in the adsorption properties of activated carbons.* Carbon, 1988. **26**(4): p. 451-459.
52. Wang, Y., et al., *Comparative studies of CO2 and CH4 sorption on activated carbon in presence of water.* Colloids and Surfaces A: Physicochemical and Engineering Aspects, 2008. **322**(1-3): p. 14-18.
53. Chue, K.T., et al., *Comparison of Activated Carbon and Zeolite 13X for CO2 Recovery from Flue Gas by Pressure Swing Adsorption.* Industrial & Engineering Chemistry Research, 1995. **34**(2): p. 591-598.
54. Jiang, L., V.G. Fox, and L.T. Biegler, *Simulation and optimal design of multiple-bed pressure swing adsorption systems.* AIChE Journal, 2004. **50**(11): p. 2904-2917.
55. Park, J.-H., J.-N. Kim, and S.-H. Cho, *Performance analysis of four-bed H2 PSA process using layered beds.* AIChE Journal, 2000. **46**(4): p. 790-802.

56. Grande, C.A. and R. Blom, *Dual Pressure Swing Adsorption Units for Gas Separation and Purification.* Industrial & Engineering Chemistry Research, 2012. **51**(25): p. 8695-8699.
57. Ruthven, D.M., *Principle of adsorption and adsorption processes*1984.
58. Fuller, E.N., P.D. Schettler, and J.C. Giddings, *New method for prediction of binary gas-phase dissusion coefficients.* Industrial & Engineering Chemistry, 1966. **58**(5): p. 18-27.
59. Poling, B., J. Prausnitz, and J.O. Connell, *The Properties of Gases and Liquids*2000: McGraw-Hill Education.
60. Lopes, F.V.S., et al., *Enhancing Capacity of Activated Carbons for Hydrogen Purification.* Industrial & Engineering Chemistry Research, 2009. **48**(8): p. 3978-3990.